In Situ Microstructural Control of Ni/Al_2O_3 and $Ni/NiAl_2O_4$ Composites from Layered Double Hydroxides

Eric D. Rodeghiero, Jungi Chisaki,† and Emmanuel P. Giannelis*

Materials Science and Engineering Cornell University, Ithaca, New York 14853-1501

Received May 30, 1996. Revised Manuscript Received November 19, 1996⊗

The transformation of Ni/Al layered double hydroxides to Ni/Al_2O_3 and $Ni/NiAl_2O_4$ composites was studied via X-ray diffraction and electron microscopy. The Ni/Al layered double hydroxide powders, with Ni^{2+}:Al^{3+} cation ratios varying from 0.5 to 3.3, were first synthesized by a coprecipitation route. The powders were then reduced in a tube furnace under hydrogen to yield Ni/Al_2O_3 or under a CO/CO_2 mixture to yield $Ni/NiAl_2O_4$. The reduced powders were uniaxially hot-pressed to form sintered pellets. In the case of the $Ni/NiAl_2O_4$ hot-pressed composites, the platelike morphology of the precursor was preserved in the final sintered microstructure. In contrast, due to the nucleation and growth mechanism that takes place in α-Al_2O_3, the Ni/Al_2O_3 hot-pressed composites exhibited no microstructural memory.

Introduction

Layered double hydroxides of various chemical systems have been extensively investigated over the past two decades.[1] Having the $[Mg_6Al_2(OH)_{16}]CO_3{\cdot}4H_2O$ or hydrotalcite structure, they can be synthesized from many different divalent/trivalent cation combinations including Mg/Al, Ni/Al, Co/Al, Ni/Cr, Co/Cr, and Ni/Fe. The general stoichiometry can be written as $[(M^{2+})_{1-x}(M^{3+})_x(OH^-)_2](A^{y-})_x{\cdot}mH_2O$, where the identity of the counterbalancing A^{y-} anion can also vary widely. Possibilities include Cl^-, NO_3^-, SO_4^{2-}, and PO_4^{3-}, but CO_3^{2-} is the most widely investigated.

Layered double hydroxides are often referred to as "anionic clays" since their structure consists of positively charged $[M_{1-x}M_x(OH)_2]^{x+}$ layers stacked parallel to each other and separated by the counterbalancing A^{y-} anions occupying the space between the layers, usually called the gallery or interlayer.[1] This is the direct opposite of smectite clays where parallel, negatively charged silicate layers are charge-balanced by gallery-occupying metal cations.

As a result of the fine scale cationic homogeneity provided by double hydroxides, much of the interest in them has centered around catalytic applications. For instance, Reichle has found heated Mg/Al layered double hydroxides to be effective catalysts for vapor-phase aldol condensation as well as other base-catalyzed polymerization reactions.[2] Double hydroxides have also been used as precursors to fine scale mixed oxide hydrogenation catalysts.[3−5] One application in this regard is the synthesis of alcohols. Finally, reduced Ni/Al layered double hydroxides, in particular, have found utility as methanation catalysts in the treatment of carbon monoxide rich gases.[6−7] In light of ever-increasing environmental restrictions, this last application is especially interesting because of the significant impact it may someday have on the state of exhaust gas regeneration technology.

Catalysis aside, other research has focused on the potential of double hydroxides to serve as precursors to high-temperature ceramic materials. Hokazono and coworkers investigated the production of $MgAl_2O_4$ (spinel) powders from hydrotalcite-like precursors and found the reactivity and sinterability of the precursor-derived powders to be high.[8] This enabled the formation of fully dense spinel monoliths without the use of sintering aids commonly necessary in conventional powder hot-pressing techniques.

In this work, we report on the synthesis and subsequent reduction of Ni/Al double hydroxide powders. Due to the homogeneous nature of the starting double hydroxide precursors, the Ni/Al_2O_3 and $Ni/NiAl_2O_4$ composites obtained after reduction exhibit nanometer size nickel particles and a high degree of dispersion between the metal and ceramic phases. Such a fine, highly dispersed nickel phase is ideal for the catalysis applications mentioned previously. In addition, hot-pressing of the reduced powders results in metal−ceramic composites (cermets) in which the high degree of dispersion between the nickel and ceramic phases is maintained. Fully sintered metal−ceramic composites have the potential to fulfill structural ceramic applications as a result of their enhanced fracture toughness and lower density as well as the ease and flexibility of their chemical synthesis.[9] Furthermore, as in the case of the $Ni/NiAl_2O_4$ composites, topotactic reactions are exploited in order to obtain in situ, highly oriented

† Present address: Toyota Automatic Loom Works Ltd., Engine Development Division, 15G, 8 Chaya Kowu Obu Aich, 474, Japan.

* To whom correspondence should be addressed.

⊗ Abstract published in *Advance ACS Abstracts,* January 1, 1997.

(1) Carrado, K. A.; Kostapapas, A.; Suib, S. L. *Solid State Ionics* **1988**, *26*, 77−86.

(2) Reichle, W. T. *J. Catal.* **1985**, *94*, 547−557.

(3) Clause, O.; Gazzano, M.; Trifiró, F.; Vaccari, A.; Zatorski, L. *Appl. Catal.* **1991**, *73*, 217−236.

(4) Courty, P.; Marcilly, C. *Preparation of Catalysts III*; Poncelet, G., Grange, P., Jacobs, P. A., Eds.; Elsevier: Amsterdam, 1983; pp 485−517.

(5) Gherardi, P.; Ruggeri, O.; Trifiró, F.; Vaccari, A.; Del Piero, G.; Manara, G.; Notari, B. *Preparation of Catalysts III*; Poncelet, G., Grange, P., Jacobs, P. A., Eds.; Elsevier: Amsterdam, 1983; pp 723−731.

(6) Kruissink, E. C.; Van Reijen, L. L.; Ross, J. R. H. *J. Chem. Soc., Faraday Trans. I*, **1981**, *77*, 649−663.

(7) Alzamora, L. E.; Ross, J. R. H.; Kruissink, E. C.; Van Reijen, L. L. *J. Chem. Soc., Faraday Trans. 1* **1981**, *77*, 665−681.

(8) Hokazono, S.; Manako, K.; Kato, A. *Br. Ceram. Trans. J.* **1992**, *91*, 77−79.

S0897-4756(96)00308-0 CCC: $14.00

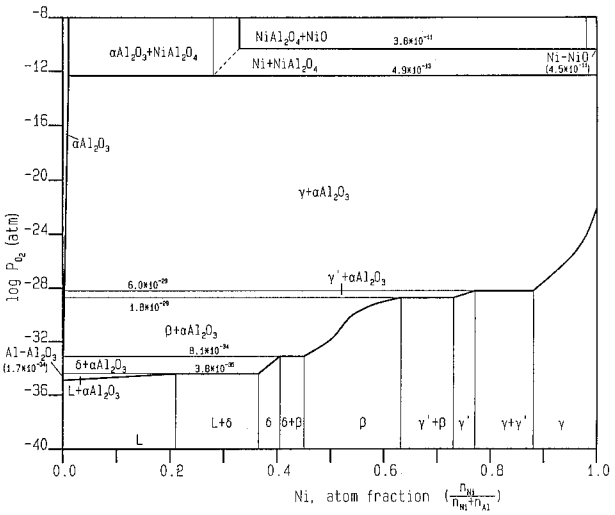

Figure 1. Ni/Al/O phase diagram for 1000 °C and 1 atm total pressure adopted from ref 14.

microstructures containing ceramic plates in a metal matrix. This added benefit of such low-cost microstructural control might further enhance the application potential of the $Ni/NiAl_2O_4$ composites, as has happened for various other in situ composite systems.[10−12] Alternatively, composites with controlled porosity may be used as desulfurizing catalysts in the refining of coal-derived gases.[13] In this latter application, composites in the form of free-standing, continuously porous billets or pellets are potential candidates.

To fully understand the differences between the Ni/Al_2O_3 and $Ni/NiAl_2O_4$ composites, both the thermodynamics of the Ni/Al/O system and the crystallography of the various phases are first reviewed.

Thermodynamics

A phase diagram for the Ni/Al/O system with the logarithm of the oxygen partial pressure on the *y*-axis is shown in Figure 1 for 1000 °C and 1 atm total pressure.[14] Note the wide range of phases that become available through a precise control of material composition and oxygen partial pressure. The two-phase regions of most interest to this work are the γ-Ni + α-Al_2O_3 and γ-Ni + $NiAl_2O_4$.

For temperatures between 850 and 1150 °C, the upper stability limit (in terms of the oxygen partial pressure) for the Ni + $NiAl_2O_4$ region (i.e., the Ni + $NiAl_2O_4$/$NiAl_2O_4$ + NiO equilibrium line) is given by[15]

$$\log(P_{O_2}) = -24478/T(\mathrm{K}) + 8.804 \pm 60/T(\mathrm{K})\ (\mathrm{atm}) \quad (1)$$

Similarly, for temperatures between 650 and 1150 °C, the upper stability limit for the Ni + α-Al_2O_3 region (i.e. the Ni + α-Al_2O_3/Ni + $NiAl_2O_4$ equilibrium line) is given as[15]

$$\log(P_{O_2}) = -25754/T(\mathrm{K}) + 7.921 \pm 60/T(\mathrm{K})\ (\mathrm{atm}) \quad (2)$$

Equations 1 and 2 show that at 1000 °C, the maximum oxygen partial pressures which can be used to reduce the Ni/Al/O system to the Ni + $NiAl_2O_4$ and Ni + α-Al_2O_3 states respectively are approximately 3.76×10^{-11} and 4.90×10^{-13} atm in agreement with Figure 1.

To achieve these oxygen partial pressures, either a H_2/H_2O or CO/CO_2 mixture can be used. In the case of the hydrogen mixture, the oxygen partial pressure can be fixed by the following equation:[16]

$$\log(P_{O_2}) \approx 2\log(P_{H_2O}/P_{H_2}) - 25700/T(\mathrm{K}) + 5.7(\mathrm{atm}) \quad (3)$$

Likewise, for the CO/CO_2 mixture, the partial pressure is given by:[16]

$$\log(P_{O_2}) \approx 2\log(P_{CO_2}/P_{CO}) - 29500/T(\mathrm{K}) + 9.1(\mathrm{atm}) \quad (4)$$

Therefore, at 1000 °C, eqs 3 and 4 indicate that the minimum required gas ratio to form Ni + α-Al_2O_3 (i.e., achieve an oxygen partial pressure of 4.90×10^{-13} atm) is 12.28 H_2:H_2O or 7.62 CO:CO_2, respectively.

Crystallography

The layered double hydroxide (LDH) structure consists of brucite-like sheets of hydroxyl octahedra sharing edges.[1] In the case of actual brucite, $Mg(OH)_2$, a divalent Mg^{2+} cation is located at the center of each octahedron. However, in LDH materials, some trivalent cations are randomly substituted for the divalent cations of the brucite structure. This substitution causes the LDH sheets to develop a net positive charge with counterbalancing anions occupying the gallery sites.

$NiAl_2O_4$ has the normal spinel structure. That is, the O^{2-} sublattice has an fcc arrangement while the Ni^{2+} cations fill $^1/_8$ of the tetrahedral sites and the Al^{3+} cations fill $^1/_2$ of the octahedral sites.[17] Therefore, a transformation from a Ni/Al double hydroxide (with Ni^{2+}:Al^{3+} = 0.5) will consist of a series of topotactic reactions in the very same manner that boehmite, a layered aluminum oxide−hydroxide material of structure somewhat similar to brucite, is known to topotactically transform to γ-Al_2O_3, a low-temperature cubic alumina which has a defect-spinel structure.[18−20] In fact, this is most likely the reason researchers have been able to produce some spinels from LDH precursors at temperatures lower than 400 °C.[21−22] That is, nucle-

(9) Rodeghiero, E. D.; Tse, O. K.; Chisaki, J.; Giannelis, E. P. *Mater. Sci. Eng.* **1995**, *A195*, 151−161.
(10) *In Situ Composites IV*; Lemkey, F. D., Kline, H. E., McLean, M., Eds.; Proceedings of the Materials Research Society; Boston, MA, 1981.
(11) Newkirk, M. S.; Urquhart, A. W.; Zwicker, H. R.; Breval, E. *J. Mater. Res.*, **1986**, *1*, 81−89.
(12) Mileiko, S. T.; Kazmin, V. I. *J. Mater. Sci.* **1992**, *27*, 2165−2172.
(13) Swisher, J. H.; Schwerdtfeger, K. *Proceedings of the Eighth Annual International Pittsburgh Coal Conference*; Pittsburgh, PA, 1991; pp 646−653.
(14) Kuznetsov, V. *Ternary Alloys*; Petzow, G., Effenberg, G., Eds.; VCH: Weinheim, FRG, 1993; Vol. 7, pp 434−440.
(15) Elrefaie, F. A.; Smeltzer, W. W. *J. Electrochem. Soc.* **1981**, *128*, 2237−2242.
(16) Gaskell, D. R. *Introduction to Metallurgical Thermodynamics*, 2nd ed.; Hemisphere: New York, 1981; pp 261−316.
(17) Kingery, W. D.; Bowen, H. K.; Uhlmann, D. R. *Introduction to Ceramics*, 2nd ed.; John Wiley & Sons: New York, 1976; pp 61−81.
(18) Brinker, C. J.; Scherer, G. W. *Sol−Gel Science*; Academic Press: San Diego, CA, 1990.
(19) Wilson, S. J.; Stacey, M. H. *J. Colloid. Interface Sci.* **1981**, *82*, 507−517.
(20) Iler, R. K. *J. Am. Ceram. Soc.* **1961**, *44*, 618−624.

ation and growth mechanisms, which typically require higher temperatures, are not necessary for the transformation.

On the other hand, α-Al_2O_3, which is the thermodynamically stable form of alumina, possesses a roughly hcp arrangement of O^{2-} anions. Therefore, a transformation from an LDH structure to a material containing α-Al_2O_3 would clearly require a nucleation and growth step, which likewise is what happens as the last step in the transformation from boehmite to α-Al_2O_3.

Experimental Procedure

Synthesis. Ni/Al layered double hydroxides were prepared by a common coprecipitation technique.[23−25] First, an aqueous solution of nickel nitrate hexahydrate and aluminum nitrate nonahydrate ($Ni(NO_3)_2{\cdot}6H_2O$ and $Al(NO_3)_3{\cdot}9H_2O$, Aldrich Chemical Co.) with a total metal cation molarity of 0.6 M was prepared. The ratio of the nickel-to-aluminum species reflected the desired cermet powder composition. Next, a second aqueous solution of sodium hydroxide (NaOH) and sodium carbonate (Na_2CO_3) was prepared. The molar amount of hydroxide used in this solution was twice that of the metal cations in the nitrate solution while the molar amount of carbonate was half that of the Al^{3+} cations in direct accordance with the double hydroxide stoichiometry $[Ni_{1-x}Al_x(OH)_2](CO_3)_{x/2}{\cdot}mH_2O$. Equal volumes of these two solutions were then simultaneously added dropwise to an additional NaOH solution at pH = 10. The volume of deionized water used in this buffer was typically twice that of either reagent solution.

The resulting mixture was then aged at 60−70 °C for 24 h. The precipitate obtained was vigorously washed with deionized water five times to completely remove all Na^+, filtered, and dried at 120 °C for 24 h. Finally, the powder was ground to 230 mesh (63 μm) with an agate mortar and pestle.

Reduction and Sintering. The reduction step was tailored to fit the nature of the final powder desired, (i.e., Ni/$NiAl_2O_4$ or Ni/Al_2O_3). In the case of Ni/Al_2O_3 powders, the LDH precursor was reduced in a quartz tube furnace under flowing 99.99% hydrogen (~20 mL/min) at a temperature of 1000 °C for 2 h. The oxygen partial pressure under these conditions was approximately 10^{-23}−10^{-24} atm as calculated by eq 3. Note that this partial pressure lies deep in the γ-Ni + α-Al_2O_3 two-phase region on the 1000 °C Ni/Al/O phase diagram. For the Ni/$NiAl_2O_4$ powders, a 1 h 1100 °C air calcination was required before reduction. The calcined powders were reduced in an alumina tube furnace at 1100 °C for 1 h in an oxygen partial pressure of $10^{-9.9}$ atm, using a flowing mixture of CO and CO_2. This partial pressure lies approximately in the middle of the γ-Ni + $NiAl_2O_4$ two-phase region at 1100 °C.

After the reduction step, all powders were handled and processed under argon to avoid reoxidation of nickel. Environmentally controlled uniaxial hot-pressing was performed on some of the reduced powders with the use of 12.7 mm (0.5 in.) inside diameter α-Al_2O_3 dies. The Ni/Al_2O_3 powders were sintered at 1400 °C for 3 h under a load of 10 MPa and an oxygen partial pressure of 10^{-12} atm in a flowing CO/CO_2 mixture. Hot-pressing of the Ni/$NiAl_2O_4$ powders was performed at 1400−1450 °C for 3 h under 10 MPa and an oxygen partial pressure of 10^{-7} atm in a flowing CO/CO_2 mixture.

After hot-pressing, the sintered pellets were removed from the dies and partitioned with the use of a circular diamond blade saw. High-quality, optically smooth surfaces were prepared by embedding portions of the pellets in Koldmount epoxy (Vernon-Benshoff Co.), coarse polishing with SiC paper, and then fine polishing with diamond paste impregnated Texmet polishing cloth (Buehler Ltd.). Finally, an aqueous ultrasonic cleaning bath was utilized immediately after polishing to remove pellet surface contamination.

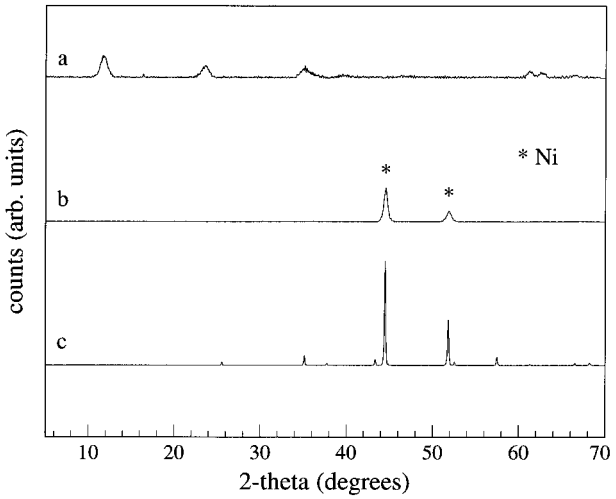

Figure 2. XRD patterns for (a) Ni/Al double hydroxide precursor with Ni^{2+}:Al^{3+} = 2, (b) same precursor after a 2 h, 1000 °C hydrogen reduction, and (c) after both reduction and a 3 h, 1400 °C uniaxial hot-pressing under 10 MPa of load.

Characterization. X-ray diffraction (XRD) was performed on a Scintag Pad X θ-θ diffractometer using Cu Kα radiation. Powder samples containing small nickel particles at varying stages of reduction/calcination were encapsulated in 1.0 mm diameter glass capillaries under argon in order to prevent reoxidation.

Transmission electron microscopy (TEM) was performed on a JEOL 1200 electron microscope at an accelerating voltage of 120 kV. Both bright-field and dark-field images as well as electron diffraction patterns were obtained. Powder samples were supported on copper grids coated with a porous polymer film. Conductive carbon overlayers were applied via sputtering.

Scanning electron microscopy (SEM) images of hot-pressed samples were obtained using a Leica 440 Stereoscan electron microscope with secondary electron and backscattered electron imaging capabilities. The accelerating voltage employed was 20 kV, and the probe current was varied between 100 and 400 pA. Densities were calculated by measuring both the mass and volume of rectangularly partitioned portions of the sintered pellets. In addition, the SEM was also used to verify the final composite compositions by performing volume fraction analysis according to ASTM 562-89. This technique was used in place of X-ray analyses such as EDS (energy-dispersive spectroscopy) due to the intrinsic difficulties of these methods, such as determining the proper matrix corrections for numerous microstructures of differing scale and morphology.[26]

Results and Discussion

Figure 2a shows the XRD pattern for a Ni/Al double hydroxide with a stoichiometry of $[Ni_{0.67}Al_{0.33}(OH)_2](CO_3)_{0.17}{\cdot}mH_2O$ (Ni^{2+}:Al^{3+} = 2). The pattern is indicative of a layered structure. The first peak corresponds to a relatively large d spacing of 7.7 Å, the (002) reflection, and the second- and third-peaks represent second and third order reflections. The smaller features at large 2θ are associated with the low-index (220) and (222) reflections. The precursor peaks are quite broad, most likely due to variations in the crystallite size and the amounts of intercalated water. Figure 2b shows the XRD pattern of a sample of the same precursor as in

(21) Gusmano, G.; Nunziante, P.; Traversa, E.; Chiozzini, G. *J. Thermal Anal.* **1991**, *37*, 1697−1707.
(22) Kannan, S.; Swamy, C. S. *J. Mater. Sci. Lett.* **1992**, *11*, 1585−1587.
(23) Reichle, W. T. *Sol. State Ionics* **1986**, *22*, 135−141.
(24) Miyata, S. *Clays Clay Miner.* **1975**, *23*, 369−375.
(25) Sato, T.; Fujita, H.; Endo, T.; Shimada, M. *React. Solids* **1988**, *5*, 219−228.
(26) Hunt, J., personal communication, 1996.

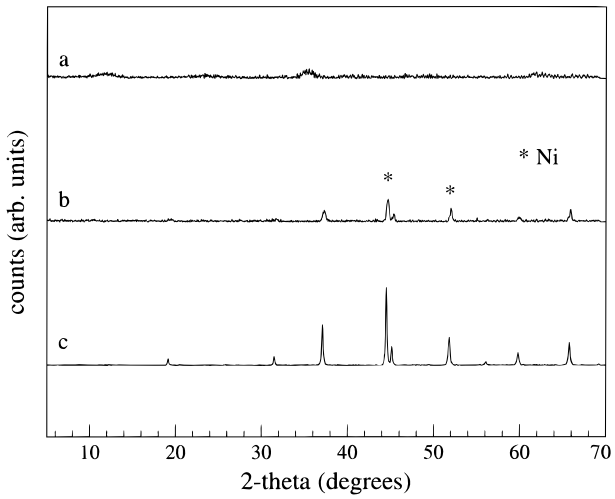

Figure 3. XRD patterns for (a) Ni/Al double hydroxide precursor with $Ni^{2+}:Al^{3+} = 1.2$, (b) same precursor after a 1 h, 1100 °C air calcination and a 1 h, 1100 °C CO/ CO_2 reduction, and (c) after both reduction and a 3 h, 1400−1450 °C uniaxial hot-pressing under 10 MPa of load.

Table 1. Summary of Precursor Compositions, Crystallinity, and Reduced Composite Volume Fractions

precursor cation ratio ($Ni^{2+}:Al^{3+}$)	precursor crystallinity (after 24 h reflux)	$Ni/\alpha\text{-}Al_2O_3$ volume composition		$Ni/NiAl_2O_4$ volume composition	
		intended	measured	intended	measured
0.5	poor[a]	20/80	22/78		
1.0	poor	33/67	29/71		
1.2	poor			20/80	21/79
2.0	moderate	50/50	not det.	35/65	38/62
3.3	good			50/50	49/51

[a] $Al(OH)_3$ also present.

Figure 2a after it has undergone the 2 h, 1000 °C hydrogen reduction used to form Ni/Al_2O_3. Note in this pattern the loss of all double hydroxide peaks and the distinct presence of nickel metal. The average grain size of the nickel at this stage, using Scherrer's equation, is approximately 35 nm.[27] No peaks attributable to the alumina are present in this pattern suggesting that the ceramic is either amorphous or in a very poorly crystalline metastable state. The stable $\alpha\text{-}Al_2O_3$ phase is not typically observed until a temperature of 1100−1200 °C, which is in good agreement with literature.[18] Finally, Figure 2c shows the XRD pattern for a sample of the same precursor as in 2a after it has undergone both the hydrogen reduction and the 3 h uniaxial hot-pressing at 1400 °C and 10 MPa to yield a Ni/Al_2O_3 pellet. The peaks attributable to Ni are still present albeit much sharper due to coarsening. The $\alpha\text{-}Al_2O_3$ phase, which accounts for the remainder of all peaks, is now also visible.

The degree of crystallinity of the LDH precursors varied with composition. This is not surprising since the layered double hydroxide structure is stable only for a certain range of $M^{2+}:M^{3+}$ cation ratios. Outside of these prescribed ranges, the double hydroxide structure may still form but only in conjunction with excess hydroxide of either the M^{2+} or M^{3+} species. In previous work, Reichle studied several LDH systems and found that pure Ni/Al hydroxide forms only when the $Ni^{2+}:Al^{3+}$ ratio is between 2 and 3.[23] For $Ni^{2+}:Al^{3+} \geq 4$, excess $Ni(OH)_2$ was present, while for $Ni^{2+}:Al^{3+} \leq 1$, excess $Al(OH)_3$ was formed.

(27) Cullity, B. D. *Elements of X-ray Diffraction*, 2nd ed.; Addison-Wesley: Reading, MA, 1978; pp 284−285.

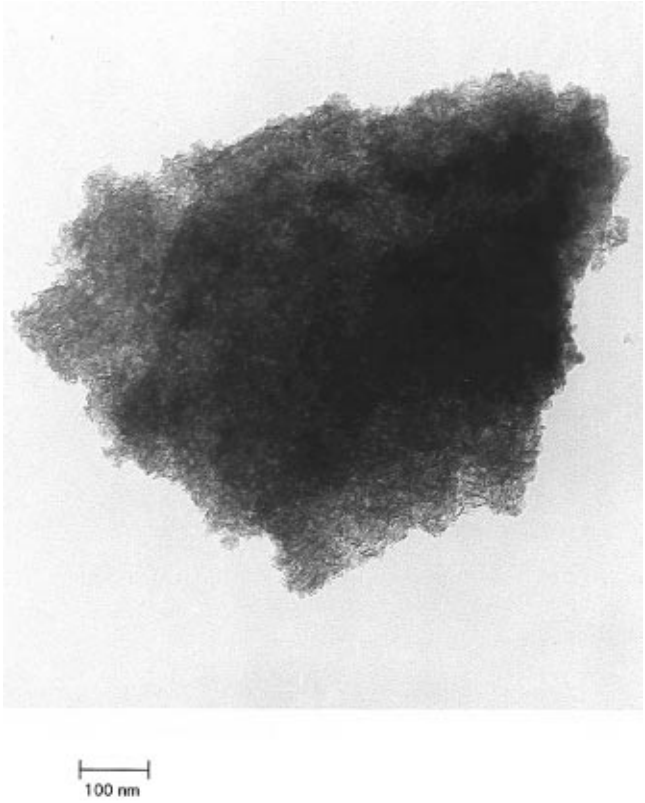

Figure 4. Bright-field TEM micrograph of a Ni/Al double hydroxide platelet with $Ni^{2+}:Al^{3+} = 2$.

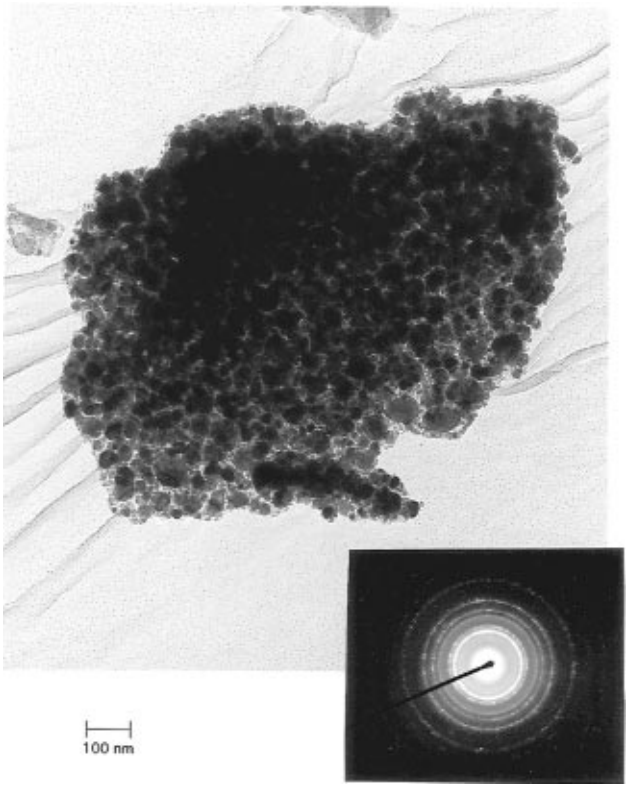

Figure 5. Bright-field TEM micrograph of a double hydroxide platelet ($Ni^{2+}:Al^{3+} = 2$) after it has undergone a 2 h, 1000 °C hydrogen reduction. Inset: associated electron diffraction pattern ($l = 60.0$ cm).

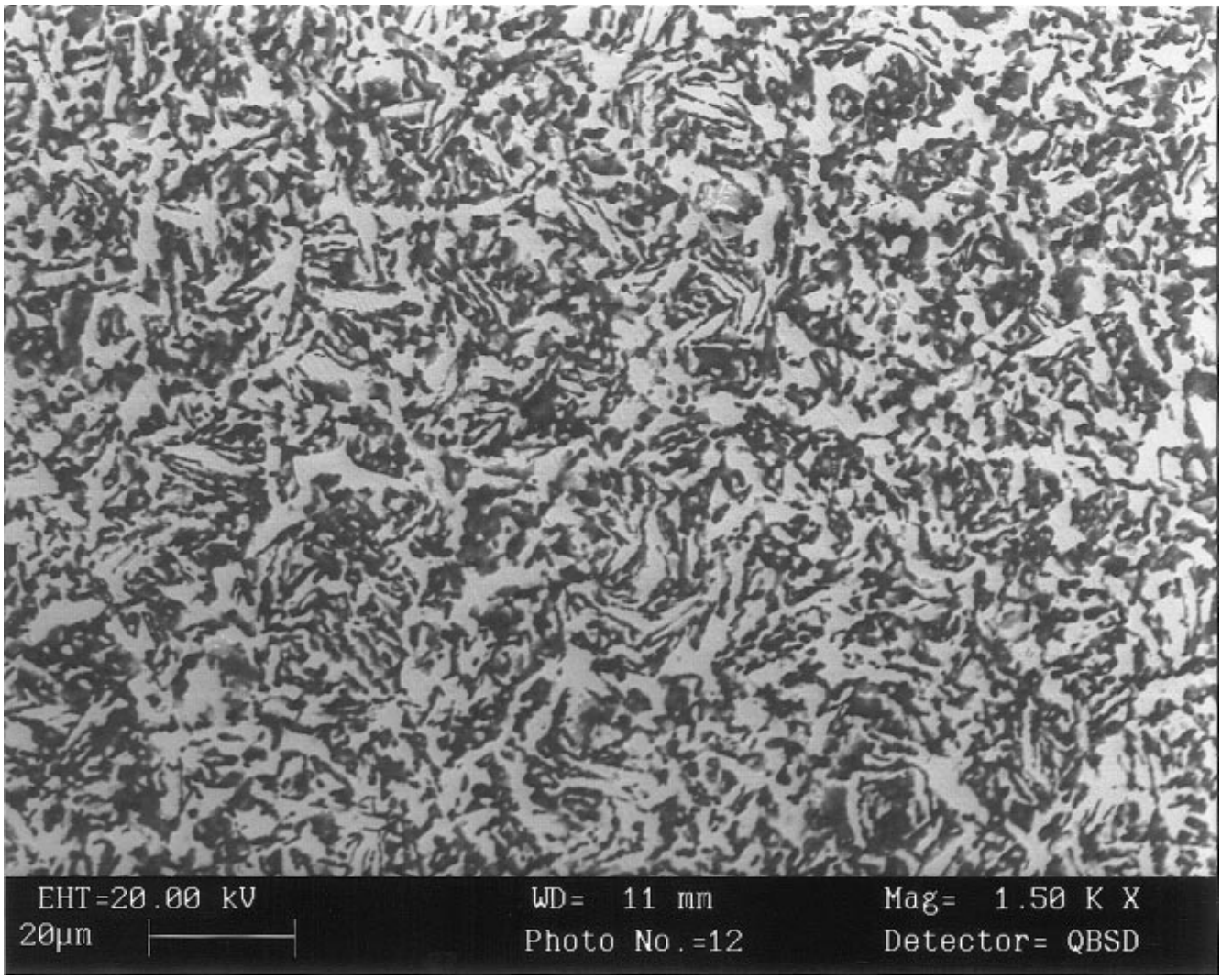

Figure 6. Top-down backscattered electron SEM micrograph of a 50/50 vol % Ni/α-Al_2O_3 hot-pressed composite (Ni = light; α-Al_2O_3 = dark).

In this work, the Ni^{2+}:Al^{3+} cation ratio was varied between 0.5 and 3.3. For Ni^{2+}:Al^{3+} ratios between 2 and 3.3, the crystallinity of the double hydroxide precursors was well developed and no excess nickel or aluminum hydroxide was observed. For Ni^{2+}:Al^{3+} ratios less than 2, the crystallinity of the double hydroxides became increasingly poor as the Ni^{2+} content decreased. However, excess $Al(OH)_3$ was not observed until the extreme Ni^{2+}:Al^{3+} ratio of 0.5.

Figure 3a shows the XRD pattern for a Ni/Al double hydroxide precursor with a stoichiometry of $[Ni_{0.55}Al_{0.45}(OH)_2](CO_3)_{0.23}\cdot mH_2O$ (Ni^{2+}:Al^{3+} ratio = 1.2). Contrast the poor crystallinity of this precursor relative to that shown in Figure 2a. The pattern for the same precursor after having undergone the 1 h, 1100 °C air calcination and 1 h, 1100 °C CO/CO_2 reduction, needed to form Ni/$NiAl_2O_4$, is shown in Figure 3b. The pattern clearly displays the presence of Ni metal. The remainder of the peaks are attributed to $NiAl_2O_4$ spinel. Interestingly, we have found that no reduction scheme to form Ni/$NiAl_2O_4$ cermet powders works consistently unless the 1 h, 1100 °C air calcination is first performed. Without this precalcination step, reduction attempts usually resulted in materials with very poor spinel crystallinity and often the presence of unknown, nonequilibrium phases, despite the use of proper thermodynamic conditions. These experiments suggest that kinetic barriers exist in the direct CO reduction of Ni/Al double hydroxide to Ni/$NiAl_2O_4$, possibly as a result of the choice of reducing agent. However these barriers can be circumvented by first producing a fully oxidized (but still topotactic) intermediate precursor. Experiments are currently underway in order to confirm this hypothesis and investigate the kinetics of the reduction reactions. Finally, Figure 3c shows the XRD pattern for a sample that has undergone both the described reduction and the 1400−1450 °C, 10 MPa uniaxial hot-pressing to form a sintered Ni/$NiAl_2O_4$ pellet. As expected, both the Ni and $NiAl_2O_4$ peaks are now more pronounced due to coarsening.

Table 1 summarizes the double hydroxide compositions investigated, their degrees of crystallinity, and the corresponding metal−ceramic compositions after reduction and hot-pressing. The double hydroxide stoichiometries have been chosen so as to provide both Ni/α-Al_2O_3 and Ni/$NiAl_2O_4$ cermets with metal-to-ceramic volume fractions of 50/50, ∼33/67 and 20/80. Note that the measured metal-to-ceramic volume fractions (according to ASTM 562-89) are in good agreement with the intended compositions.

TEM studies show that the LDHs are composed of platelike particles with large aspect ratios and often hexagonal shapes. The width of the plates varies widely from 0.5 μm to as large as 30 μm, and though possible,

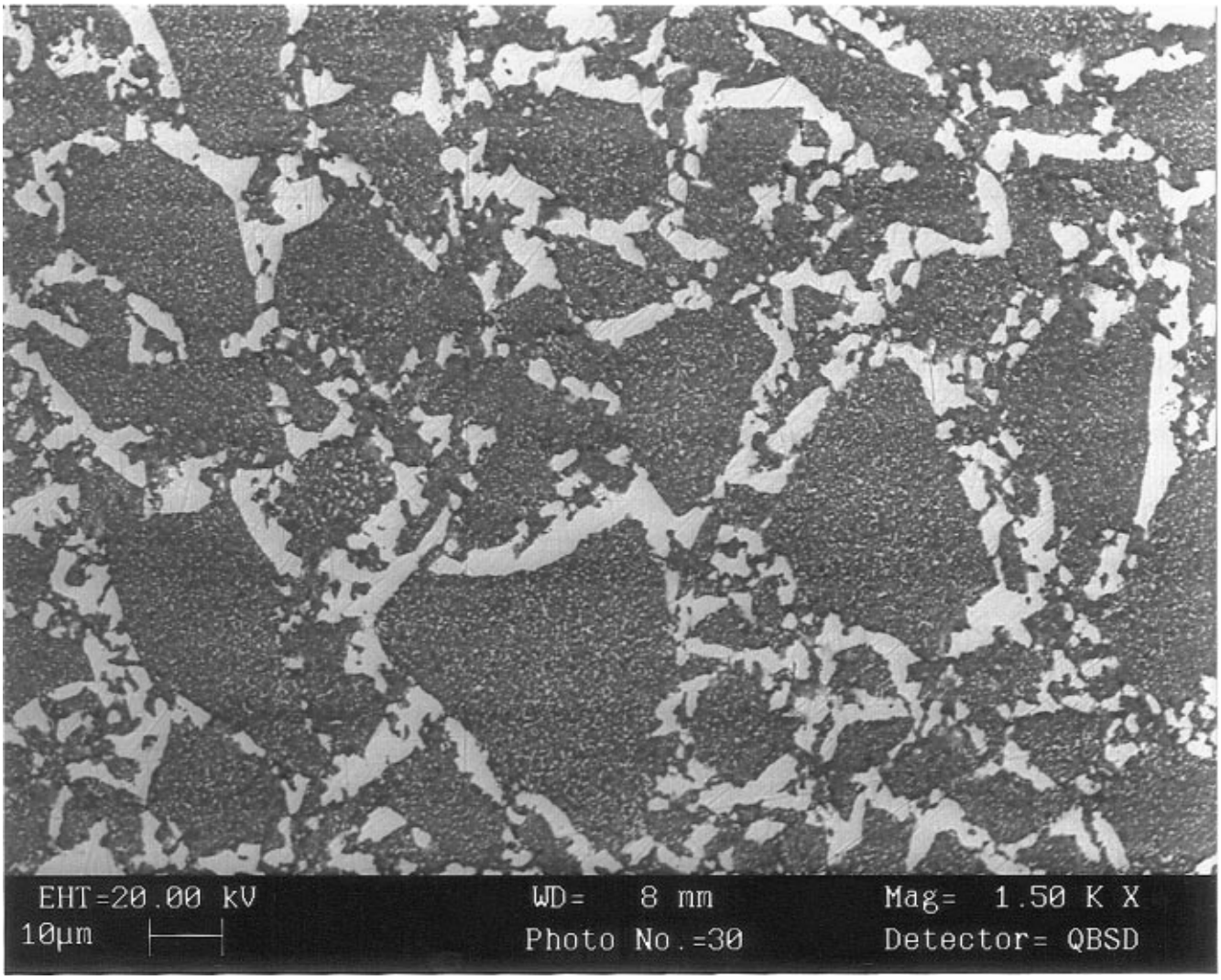

Figure 7. Top-down backscattered electron SEM micrograph of a 33/67 vol % $Ni/NiAl_2O_4$ hot-pressed composite (Ni = light; $NiAl_2O_4$ = dark).

no efforts have yet been made to precisely control the size of the LDHs. Figure 4 is a bright-field TEM micrograph of a Ni/Al LDH particle with $Ni^{2+}:Al^{3+} = 2$. The particle is platelike and appears homogeneous throughout.

Figure 5 is a bright field TEM micrograph of the same precursor as in Figure 4 after it has undergone hydrogen reduction to form Ni/Al_2O_3. Although the particle shown has remained platelike, the interior structure of the particle has clearly been altered. In particular, the particle seems to have separated into a matrix phase (light contrast) and a precipitated phase (dark contrast). The corresponding electron diffraction pattern is shown on the same figure. Indexing of this pattern reveals the presence of Ni metal. The nickel particles are roughly spherical and vary between 20 and 60 nm in size, in agreement with the X-ray observations. Electron diffraction also confirms the absence of any crystalline ceramic phase in agreement with the XRD which shows nickel metal as the only crystalline phase after hydrogen reduction for 2 h at 1000 °C. Recall that α-Al_2O_3 will not form at 1000 °C.

TEM studies of the LDHs which underwent the calcination and reduction to form $Ni/NiAl_2O_4$ powders yield similar results. That is, upon reduction, the precursor particles are found to undergo a fine-scale phase separation while simultaneously maintaining their platelike structure.

Figure 6 shows a top-down backscattered electron SEM micrograph of a 50/50 vol. % Ni/α-Al_2O_3 hot-pressed composite. A high degree of dispersion between the metal and ceramic phases is seen. This fine dispersion is most likely a result of the highly homogeneous LDH precursors. However, there seem to be no remains of the reduced platelike particles observed in TEM (Figure 5). This observation is typical for all of the Ni/α-Al_2O_3 hot-pressed composites regardless of composition. Since the transformation to α-Al_2O_3 by nucleation and growth is not a topotactic reaction, the shape of the original platelike particles is lost during hot-pressing. That is, as the α-Al_2O_3 phase nucleates during hot-pressing, the subsequent growth of the ceramic domains is not correlated with the orientation of the original platelike particles.

In contrast, in $Ni/NiAl_2O_4$ hot-pressed composites, the morphology of the initial reduced platelets is, to varying degrees, preserved in the sintered microstructure. Figure 7 shows a top-down backscattered electron SEM micrograph of a 33/67 vol % $Ni/NiAl_2O_4$ hot-pressed composite. The micrograph reveals the presence of platelike spinel structures which contain small nickel particles (nanometer scale) and are embedded in a

second, coarser nickel phase (micron scale). For Ni/$NiAl_2O_4$ hot-pressed composites of higher metal content than 33 vol %, the platelike microstructure, while still present, is not as well developed as in Figure 7 since large quantities of precipitated metal disrupt the interior of the plate structures. However, for Ni/$NiAl_2O_4$ composites of nickel content lower than 33 vol %, the platelike microstructure is even more apparent.

This microstructural "memory" of the Ni/$NiAl_2O_4$ system is most likely a result of the topotactic nature of all ceramic transformations from the initial LDH precursors through the final $NiAl_2O_4$ spinel phase. This contrasts sharply with the Ni/α-Al_2O_3 composites where transitions between the metastable cubic alumina phases involve topotactic transformations, but a nucleation and growth mechanism is required to produce the final α-Al_2O_3 phase. Since the hexagonal α-Al_2O_3 does not form until the powder is compacted and in the hot-pressing stage, the α-Al_2O_3 grains which form under the 10 MPa of pressure can grow in any direction regardless of the initial platelike powder morphology.

These differences between the Ni/Al layered double hydroxide transformations to $NiAl_2O_4$ and α-Al_2O_3 have significant implications. Most notably, the topotactic nature of the LDH/spinel transformation suggests the potential for varying the morphology of Ni/$NiAl_2O_4$ sintered composites by simply varying the initial LDH powder morphology. Furthermore, ways of precisely controlling the size and shape of such LDH powder particles are well documented though not yet attempted in this work.[23,28] Such an in situ microstructural control over the composite microstructure may be highly beneficial to the optimization of the cermet's fracture properties. Furthermore, the wide range of layered double hydroxide and spinel systems available suggests that the very same type of topotactic transformations may be applied to exercise microstructural control over other metal/spinel systems as well (with alloys such as Co/Ni or Ni/Fe also as potential metallic phase candidates).

(28) Hansen, H. C. B.; Taylor, R. M. *Clay Miner.* **1990**, *25*, 161–179.

Conclusions

Ni/Al_2O_3 and Ni/$NiAl_2O_4$ composites were prepared by controlled reduction of Ni/Al layered double hydroxides. The reduced powders retained the platelike morphology of the initial double hydroxide precursors as a result of the topotactic transformations involved in reaching either the $NiAl_2O_4$ or metastable cubic alumina matrix phase. Both the powders and the hot-pressed samples displayed a high degree of dispersion between the metal and ceramic phases due to the atomic homogeneity of the starting precursors. Furthermore, in the case of Ni/$NiAl_2O_4$ hot-pressed composites, the platelike morphology of the initial powders was preserved in the final sintered microstructures especially for composites containing relatively low metal contents. This in situ microstructural control leads to both nanometer-scale and micron-scale nickel regions in the form of Ni-containing $NiAl_2O_4$ platelets in a Ni matrix. Work is presently underway to both evaluate the mechanical properties of these Ni/$NiAl_2O_4$ composites and vary the scale of their unique morphology by precisely controlling the size and shape of the initial layered double hydroxide precursors.

Acknowledgment. Supported by the Air Force Office of Scientific Research under Grant No. F49620-93-1-0235 and the Office of Naval Research under Grant No. N00014-92-J-1526. E.D.R. acknowledges the support of a DoD fellowship. This study benefited from the use of MRL Central Facilities funded by the National Science Foundation.

CM960308I